Topographic Amplification of Tectonic Displacement: Implications for Geodetic Measurement of Strain Changes

DAVID F. McTIGUE

Fluid Mechanics and Heat Transfer Division I, Sandia National Laboratories

ROSS S. STEIN

U.S. Geological Survey

Correlations of level changes with topography demand an assessment of the effect of an irregular free boundary on surface deformation. This is examined through a plane strain elastic model with topography of small slope, subjected to a change in the far-field horizontal stress. To leading order, vertical surface displacements due to the topographic perturbation are proportional to the local relief. Elevation-dependent uplift results from a compressional change, and downdrop results from a tensional change. The model further predicts that the ratio of elevation change to elevation is proportional to and of the same order of magnitude as the regional strain. Horizontal strains are locally perturbed by topography as well, with the magnitude scaling with the local slope. The predicted localization of level changes is very small in aseismic regions and cannot contribute significantly to measured correlations. A test case in southern California bears this out, with strains of order 10^{-6} accompanied by elevation change to elevation ratios of order 10^{-4}. Releveling following the Nankaido-Tonankai earthquakes, which induced large coseismic and postseismic strains, reveals scattered examples of elevation-dependent level changes. However, when compared to modeled strains, the correlations are again at least an order of magnitude larger than the localization effect predicted by the elastic model. Although the topographic perturbation of vertical displacements appears to be unmeasurably small, local variations in horizontal strain or borehole dilatation across steep relief may be discernible with current technology.

INTRODUCTION

Geodetic measurements of surface displacements and strain provide crucial data used to infer changes in the state of stress in the earth's crust. Locally, surface deformation will vary in the presence of irregular topography. We explore in this paper the form and magnitude of these variations and their significance in the interpretation of geodetic data.

The principal impetus for this study derives from widespread observations of leveling anomalies that are strongly associated with topography. Correlations between geodetically measured tilt and terrain slope have been noted in many tectonically active regions. Examples have been cited in Israel [*Karcz and Kafri*, 1971], the Appalachians [*Brown and Oliver*, 1976; *Citron and Brown*, 1979], California [*Jackson et al.*, 1980], and Japan (this paper). In all of these cases, observed changes from releveling exhibit a strong correlation with topography. Both positive correlations, in which topographic highs undergo apparent uplift, and negative correlations, in which topographic highs are displaced downward, are commonly noted. An illustration of this phenomenon, showing the apparent change in elevation for bench marks along a traverse in southern California, reported in part by *Prescott and Savage* [1976], is shown in Figure 1. Elevation changes appear to be proportional to elevation, and the correlation changes from negative over the period 1971–1973 to positive over the interval 1973–1978.

Such correlations have recently received a great deal of attention because of their importance in the interpretation of southern California leveling [e.g., *Castle et al.*, 1976; *Jackson et al.*, 1980; *Mark et al.*, 1981; *Reilinger*, 1980; *Rundle and McNutt*, 1981; *Stein*, 1981]. To date, most analyses of slope-dependent correlations in leveling have focused on sources of systematic measurement errors. Indeed, these investigations have revealed significant errors due to miscalibration of rods, atmospheric refraction, and other causes. Nonetheless, little attention appears to have been accorded to the possibility that some of the observed correlations may reflect true tectonic deformation that results from the localization of displacements in steep terrain. In this paper, we present a simple model and test cases designed to obtain a first-order estimate of such real topographic effects.

Analysis based on an elastic model yields predictions for the topographic perturbation of both leveling and strain measurements. A correlation of elevation change and elevation is predicted, but the ratio of the two is of the order of the regional strain change. Thus, although the effect qualitatively resembles the observed phenomenon, it is very small for typical aseismic deformation. For this reason, we examine the large strains associated with the Tonankai and Nankaido, Japan, earthquakes of 1944 and 1946 and level changes accompanying them. Tilt/slope correlations identified in these data are at least an order of magnitude larger than predicted by the model, and we conclude that the elastic localization effect, if present, is masked by other phenomena.

Topographic modification of regional strain is of the order of the local slope and thus may be measurable. We know of no existing data against which to test this prediction.

TOPOGRAPHIC MODIFICATION OF TECTONIC STRESS

McTigue and Mei [1981] have presented an approximate analytical approach to the effect of an irregular free surface on gravity-induced stresses in the uppermost lithosphere. They also showed briefly how the method can be extended to topographic modification of tectonic stress, modeled as a uniform

far-field compression or tension. We extend this result to consider the displacement field associated with a change in the far-field load. Because details of the tectonic stress problem were omitted by McTigue and Mei [1981] and are central to the present developments, we outline the solution here.

Assume plane strain of an elastic half space with an irregularly shaped free surface defined by some function $h(x)$ (Figure 2). The region is subject to a uniform far-field "tectonic stress" change, such that

$$\sigma_{0xx} = \pm\sigma_\infty = \text{const} \qquad (1)$$

where the plus or minus correspond to tensional or compressional stress changes, respectively. We wish to determine the departure from this uniform stress state caused by the topography, $h(x)$.

The surface relief $h(x)$ is assumed to be characterized by a horizontal length scale, L, and a vertical length scale, H, such that $H/L = \varepsilon \ll 1$. Thus ε is a characteristic slope. The analysis is a perturbation scheme that yields approximate solutions with an error of order ε^2; for a characteristic slope $\varepsilon = 0.1$, the error is of the order of 1%. The approximation is particularly good for topographic profiles following level lines, insofar as most leveling is accomplished over slopes less than 0.05.

The assumption of a semi-infinite region limits the applicability of the model to topography with L of the order of the elastic thickness of the lithosphere or smaller [McTigue and Mei, 1981]. For larger L the influence of boundary conditions at the base of the lithosphere becomes important. Thus the model is constrained to the examination of topographic features with horizontal length scales of tens of kilometers or less. This is, in fact, the scale at which apparent topographic effects on leveling have caused the greatest concern [e.g., Jackson et al., 1980].

According to the foregoing scaling arguments, we normalize the coordinates x and y by L, the surface geometry h by H, and the stress σ by σ_∞. The dimensionless far-field stress then becomes $\sigma_{0xx} = \pm 1$, and the free surface is defined at $y = \varepsilon h(x)$. We define a stress potential, ϕ, representing the departure from the uniform stress state due to the topography such that
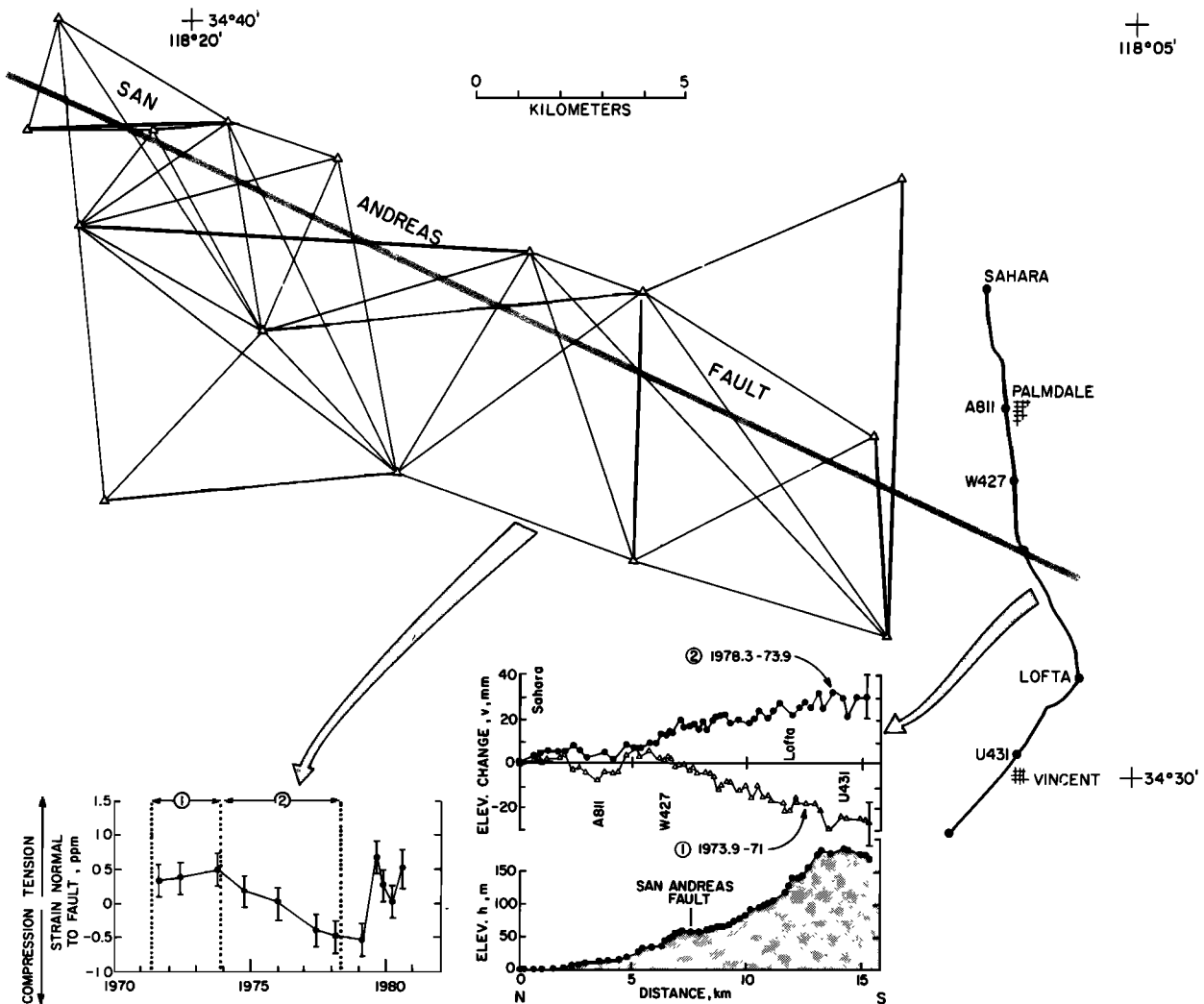
$$\sigma_{xx} = \pm 1 + \phi_{,yy} \qquad (2a)$$

Fig. 1. Vincent-Sahara level line and adjacent strain net, southern California. Strain normal to the fault trace, averaged over the net, shows extension from 1971 to 1973 and compression from 1973 to 1978. Measured vertical displacements are roughly proportional to elevation and exhibit downdrop during extensional strain changes and uplift during compressional changes. Ratio of elevation change to elevation is of order 10^{-4}; strain change is of order 10^{-6}.
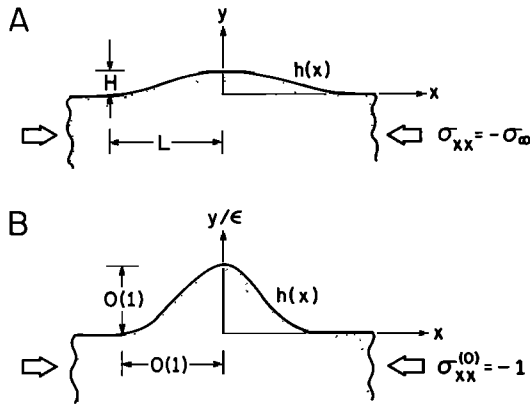
A

B

Fig. 2. Definition sketch for region with topography under far-field load. (a) Physical variables. $H/L = \varepsilon \ll 1$. (b) Dimensionless variables showing "stretched" y.

$$\sigma_{yy} = \phi_{,xx} \tag{2b}$$

$$\sigma_{xy} = -\phi_{,xy} \tag{2c}$$

where commas denote differentiation with respect to the succeeding spatial variables. Equations $(2a)$–$(2c)$ satisfy equilibrium identically and give, with the compatability equation,

$$\nabla^4 \phi = 0 \tag{3}$$

The free surface boundary conditions are given by

$$\sigma_{xy} = \varepsilon\sigma_{xx}h_{,x} + O(\varepsilon^2) \qquad y = \varepsilon h$$
$$\sigma_{yy} = \varepsilon\sigma_{xy}h_{,x} + O(\varepsilon^2) \qquad y = \varepsilon h \tag{4}$$

We assume that ϕ can be written as a series in powers of ε:

$$\phi = \varepsilon\phi^{(1)} + \varepsilon^2\phi^{(2)} + \cdots \tag{5}$$

Now, substituting (2) into (3) and (4), expanding about $y = 0$, introducing (5), and collecting like powers of ε, we obtain the order ε boundary value problem:

$$\nabla^4\phi^{(1)} = 0 \tag{6a}$$

with

$$\phi_{,xy}^{(1)}(x, 0) = \mp h_{,x} \tag{6b}$$

$$\phi_{,xx}^{(1)}(x, 0) = 0 \tag{6c}$$

This simply states that the leading order effect of the topography is equivalent to a distributed shear traction on a plane boundary and the shear is proportional to the local topographic slope (Figure 3).

The problem stated in (6) can be solved in some generality by the method described by Sneddon [1951]. Transforming (6), we obtain

$$\bar{\phi}_{,yyyy}^{(1)} - 2\zeta^2\bar{\phi}_{,yy}^{(1)} + \zeta^4\bar{\phi}^{(1)} = 0 \tag{7a}$$

with

$$\bar{\phi}_{,y}^{(1)}(0) = \mp\bar{h} \tag{7b}$$

$$\bar{\phi}^{(1)}(0) = 0 \tag{7c}$$

where overbars indicate the Fourier transforms,

$$\bar{f} = \int_{-\infty}^{\infty} fe^{i\zeta x}dx$$

The solution satisfying (7) and vanishing as $y \to -\infty$ is

$$\bar{\phi}^{(1)} = \mp\bar{h}ye^{|\zeta|y} \tag{8}$$

Expanding the stresses (2) about $y = 0$, using (5), and substituting from (8), we obtain for the near-surface stresses (y of order ε)

$$\sigma_{xx} = \pm\left[1 - \varepsilon\frac{1}{\pi}\int_{-\infty}^{\infty}|\zeta|\bar{h}e^{-i\zeta x}\,d\zeta\right] + O(\varepsilon^2) \tag{9a}$$

$$\sigma_{yy} = 0 + O(\varepsilon^2) \tag{9b}$$

$$\sigma_{xy} = \pm\varepsilon h_{,x} + O(\varepsilon^2) \tag{9c}$$

which is the result presented previously by McTigue and Mei [1981]. Note that the vertical variation of the near-surface stress is a higher-order effect so that there is no y dependence in (9).

The Displacement Field

We now turn to the displacements associated with the foregoing stress field. Dimensionless displacements are introduced by normalizing to the characteristic length $\sigma_\infty L/E$, where E is Young's modulus.

Note that the displacement, $u^{(0)}$, due to the far-field tectonic stress, $\sigma^{(0)} = \pm 1$, are indeterminate. This is an artifact of the half-space assumption; a small stretching integrated over an infinite region yields infinite displacements. We shall assume that this difficulty can be resolved by a more elaborate model for the far-field stress that accounts for a lithosphere of finite thickness but that the driving stress for the perturbation is reasonably well represented by (1). Thus we confine our attention here to the displacements associated with the perturbation due to topography only, $\varepsilon u^{(1)} + O(\varepsilon^2)$.

It can be shown [Sneddon, 1951] that the displacements associated with a stress potential ϕ are given by

$$u = \frac{i(1 + \nu)}{2\pi}\int_{-\infty}^{\infty}[(1 - \nu)\bar{\phi}_{,yy} + \nu\zeta^2\bar{\phi}]e^{-i\zeta x}\frac{d\zeta}{\zeta} \tag{10}$$

$$v = \frac{1 + \nu}{2\pi}\int_{-\infty}^{\infty}[(1 - \nu)\bar{\phi}_{,yyy} - (2 - \nu)\zeta^2\bar{\phi}_{,y}]e^{-i\zeta x}\frac{d\zeta}{\zeta^2} \tag{11}$$

Now, in the near-surface region (y of order ε),

$$u - u^{(0)} = \varepsilon u^{(1)}(x, 0) + O(\varepsilon^2)$$
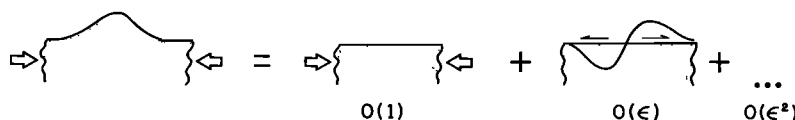$$v - v^{(0)} = \varepsilon v^{(1)}(x, 0) + O(\varepsilon^2) \tag{12}$$

Fig. 3. Sketch illustrating perturbation scheme. Far-field compression across a region with topography is approximated by uniform compression across a half space, modified by a distributed shear traction at order ε. Traction is proportional to topographic slope. Higher-order effects are neglected.

Using (8) in (10) and (11) and noting (12), we obtain the principal result of this analysis:

$$u - u^{(0)} = \mp \varepsilon(1 - v^2)\frac{i}{\pi}\int_{-\infty}^{\infty}(\text{sgn }\zeta)\bar{h}e^{-i\zeta x}\,d\xi + O(\varepsilon^2) \qquad (13)$$

$$v - v^{(0)} = \mp \varepsilon(1 + v)(1 - 2v)\frac{1}{2\pi}\int_{-\infty}^{\infty}\bar{h}e^{-i\zeta x}\,d\xi + O(\varepsilon^2) \qquad (14a)$$

$$v - v^{(0)} = \mp \varepsilon(1 + v)(1 - 2v)h + O(\varepsilon^2) \qquad (14b)$$

We are able to invert (14a) directly as indicated in (14b). Equation (14b) is particularly important. It states that a change in the far-field stress results in a contribution to the vertical displacements that is proportional to the local topographic height. We emphasize that the result is obtained for arbitrary geometry, provided that the characteristic slope is small.

In order to test the predictions of (13) and (14b), it is convenient to return to dimensional form and to replace the driving stress, $\sigma_{xx}^{(0)}$, by $[E/(1 - v^2)]e_{xx}^{(0)}$. Thus the topographic perturbation of the horizontal strain, obtained by differentiating (13), and the local variation of the vertical displacement are related to the directly measurable regional strain $e_{xx}^{(0)}$ by

$$\frac{e_{xx}^{(1)}}{e_{xx}^{(0)}} = -\frac{1}{\pi}\int_{-\infty}^{\infty}|\xi|\bar{h}e^{-i\zeta x}\,d\xi + O(\varepsilon^2) \qquad (15)$$

$$\frac{v^{(1)}}{h} = \left(-\frac{1 - 2v}{1 - v}\right)e_{xx}^{(0)} + O(\varepsilon^2) \qquad (16)$$

Equation (15) shows that the topography gives rise to local departures from the regional strain of the order of the charac-
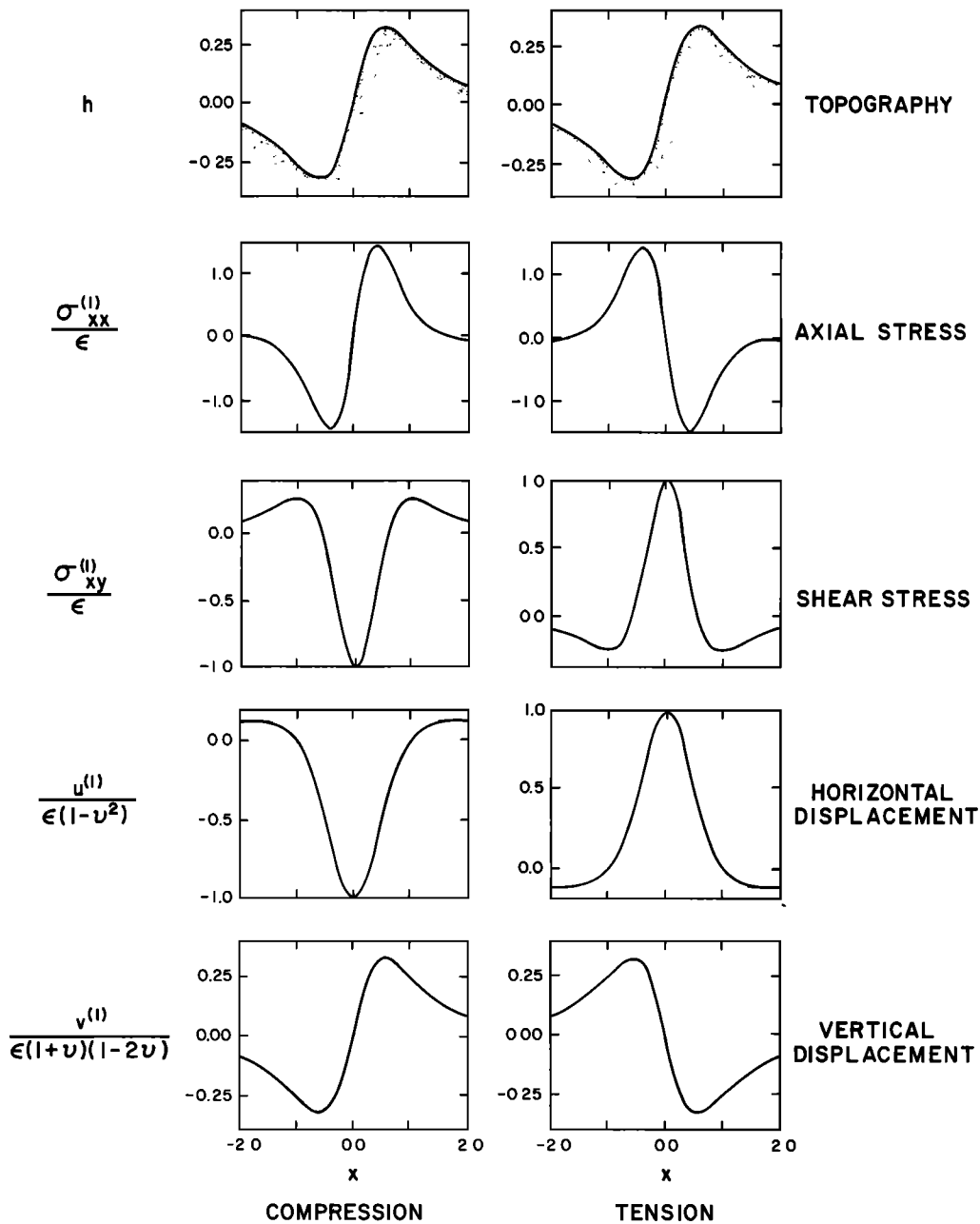

Fig. 4. Example of dimensionless perturbation stress and displacement fields due to an adjacent valley and ridge (equations (17)–(21)). Note, in particular, the vertical displacements $v^{(1)}$ in comparison to topography h.
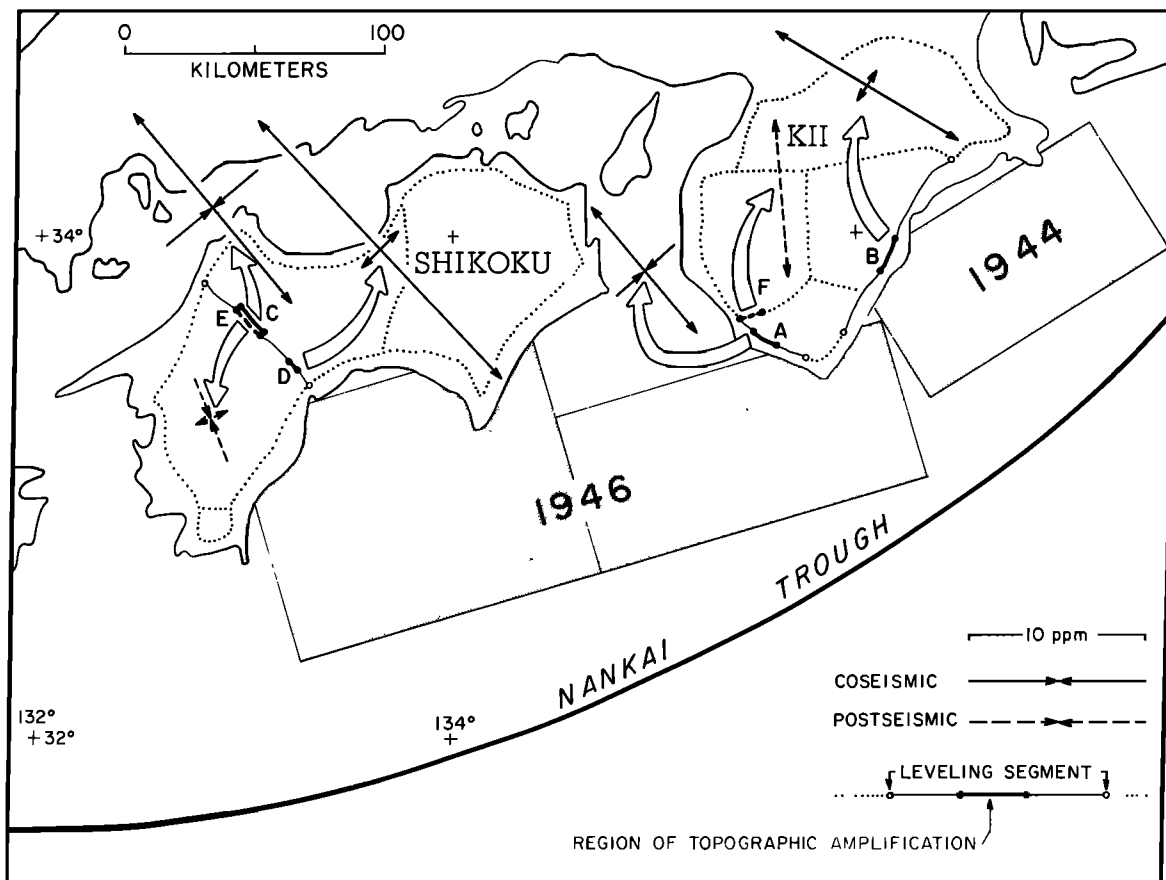
Fig. 5. Region of Tonankai and Nankaido earthquakes, Japan. Shaded areas indicate modeled fault planes (Table 1). Modeled principal strains (Table 2) shown for six localities exhibiting tilt/slope correlations.

teristic slope, H/L. The ratio of elevation change to elevation (equation (16)) is proportional to the regional strain and of the same order of magnitude. For example, if $v = 1/4$, the constant of proportionality is $(-2/3)$.

EXAMPLE

The above results are more easily envisioned through a simple example for which explicit expressions can be computed. Consider an adjacent ridge and valley defined by

$$h(x) = x(a^2 + x^2)^{-2} \qquad (17)$$

where $a = $ const. For tension/compression we find from (9a), (9c), (13), and (14b):

$$\sigma_{xx} = \pm\left[1 - \varepsilon\frac{2x(3a^2 - x^2)}{a(a^2 + x^2)^3}\right] + O(\varepsilon^2) \qquad (18)$$

$$\sigma_{xy} = \pm\varepsilon\frac{a^2 - 3x^2}{(a^2 + x^2)^3} + O(\varepsilon^2) \qquad (19)$$

$$u - u^{(0)} = \pm\varepsilon(1 - v^2)\frac{a^2 - x^2}{a(a^2 + x^2)^2} + O(\varepsilon^2) \qquad (20)$$

$$v - v^{(0)} = \mp\varepsilon(1 + v)(1 - 2v)\frac{x}{(a^2 + x^2)} + O(\varepsilon^2) \qquad (21)$$

Equations (17)–(21) are shown in Figure 4 with $a = 1$ (ε in this case is identified with the maximum slope). Note also that e_{xx} varies like (18).

Both compressional and tensional stress changes are illus-

trated. The correlation of vertical displacement $v^{(1)}$ and elevation h is easily seen in Figure 4. The correlation is positive for an increase in the far-field compression and negative for a relative decrease ("relaxation").

THE VINCENT-SAHARA LINE

Equation (14b) shows that the localization of near-surface stress and deformation by topography results in a correlation of elevation change and elevation resembling, at least in form, that which is widely observed [e.g., Jackson et al., 1980]. The model is appealing in that it directly addresses two features often cited as suggestive of measurement error: (1) the observation of correlations at small lateral length scales of the order of kilometers, and (2) the observation of both positive and negative correlations, often in the same area (see Figure 1).

Encouraged by these qualitative features captured by the model, we seek a situation for which a quantitative test is possible using (16). This requires simultaneous and independent leveling and strain data, which are quite scarce. We have identified one locality in southern California that provides a test case. A level line from Vincent to Sahara was surveyed in 1971, 1973 [Prescott and Savage, 1976], and 1978 (National Geodetic Survey, Southern California Releveling Program, unpublished data, 1979). The line runs perpendicular to a long ridge with about 200 m of relief. Because leveling performed after 1970 utilized relatively short and uniform sight lengths, the elevations should be subject to minimal refraction error, which is proportional to the square of the sight length.

TABLE 1. Model Fault Parameters

Earthquake	M_w	Length, km	Width, km	Dip, deg	Dip/Right Lateral Slip	Coseismic Slip, m	Postseismic Slip, m
1946 Nankaido	8.1						
West		150	100	20	2:1	6.0	2.2
East		150	70	25	2:1	4.0	2.2
1944 Tonankai	8.1	130	70	25	3:1	4.0	0.0

Magnitude from *Kanamori* [1977].

During the period 1971–1973, the line exhibited elevation-dependent downdrop, whereas it shows elevation-dependent uplift from 1973 to 1978 (Figure 1). The ratio of elevation change to elevation is of the order of 10^{-4}. An extensive strain net was monitored over this same period in an area adjacent to the level line [*Savage et al.*, 1981]. The second releveling interval (1973–1978) encompasses a period of compression parallel to the Vincent-Sahara level line. The observed pattern from 1971 to 1978 is qualitatively in accord with the elastic model: A negative tilt/slope correlation was measured during a period of possible line-parallel extension, and a positive correlation was noted during a period of compression. Quantitatively, however, the model prediction is not borne out. The strains measured during this period were of the order of 10^{-6}, two orders of magnitude smaller than the observed values of $v^{(1)}/h$.

In fact, it is quite evident that a large $v^{(1)}/h$ such as that measured along the Vincent-Sahara line can not be a result of the elastic deformation considered in the model because aseismic strains of that order (cf. equation (16)) are unreasonably large. Indeed, the predicted phenomenon is very small in a typical southern California setting. Even for a rapid aseismic strain rate of 10^{-6} yr^{-1} and pronounced topography of $h \sim 10^3$ m, one would have to discriminate a perturbation displacement $v^{(1)}$ of only 1 mm after 1 year to detect the predicted correlation.

The Nankaido and Tonankai Earthquakes

It is apparent that if the relationship given by (16) is to be measurable in the field, it must be sought in a region that has undergone very large strains. We consider here the changes associated with the great subduction earthquakes of the Nankai trough, Japan, where the Philippine Sea plate descends beneath the continental Asian plate (Figure 5). Extensive leveling data are available for the area affected by these events. Direct strain measurements were not made, but the strains can be modeled with some confidence.

The Tonankai and Nankaido earthquakes of 1944 and 1946 ruptured 430 km of the plate boundary. The seismic and geodetic fault parameters for these earthquakes have been widely investigated [*Fitch and Scholz*, 1971; *Fitch*, 1972; *Kanamori*, 1972; *Ando*, 1975; *Thatcher and Rundle*, 1979]. Because of excellent seismic observations of the main shocks and aftershocks, tsunami arrivals and heights, horizontal shear strains, tide gage records, and coastal releveling, the coseismic dislocations can be unusually well constrained. *Ando* [1975] synthesized the coseismic data and found that the fault slip is consistent with the direction of plate motion obtained by *McKenzie and Parker* [1967] and *Minster and Jordan* [1978].

Using the fault parameters supplied by *Ando* [1975], we calculate the surface strain field in coastal Japan produced by
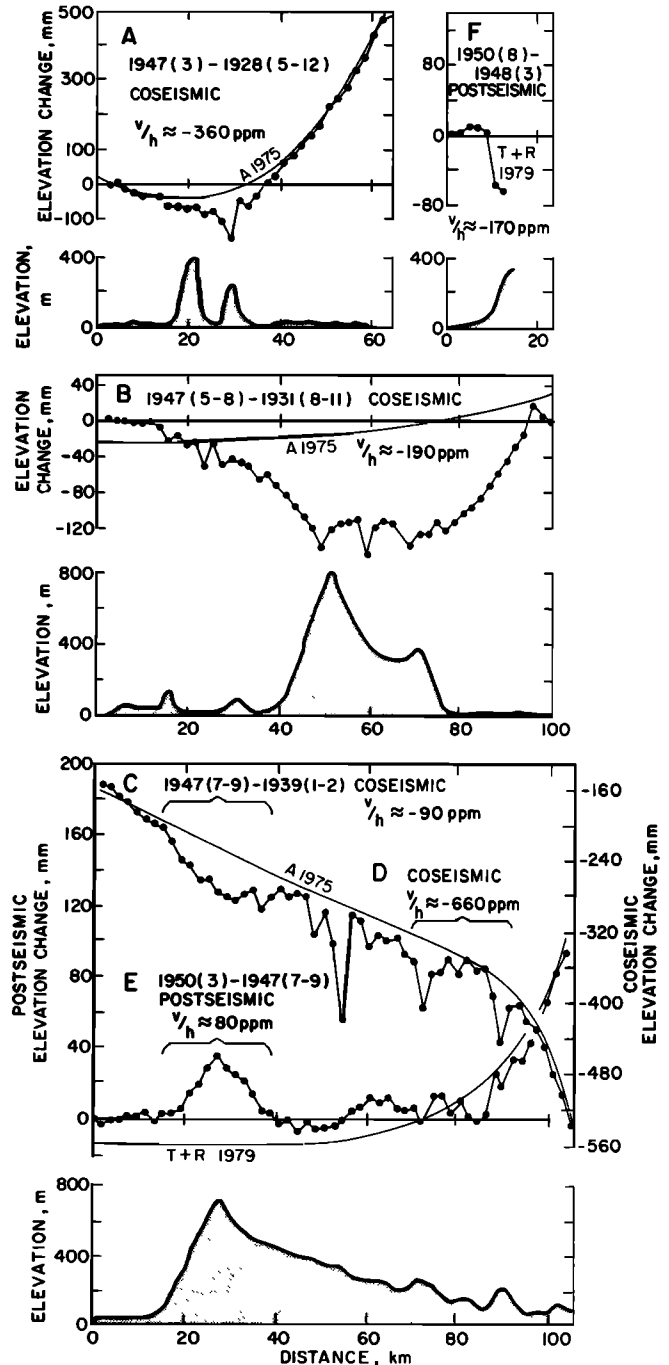

Fig. 6. Elevation changes and topography for level line segments in the Tonankai-Nankaido area (see Figure 5). Calculated displacements from *Ando* [1975] and *Thatcher and Rundle* [1979] are shown to emphasize regional deformation neglecting local topographic effects.

TABLE 2. Slope-Dependent Correlations

Site	Coseismic/ Postseismic	Length, km	Mean Slope	$v^{(1)}/h$, ppm	Axial Strain $e_{xx}^{(0)}$, ppm	Normal Strain $e_{zz}^{(0)}$, ppm	Normal/Axial Strain $\lvert e_{zz}^{(0)}/e_{xx}^{(0)} \rvert$	$\dfrac{v^{(1)}/h}{e_{xx}^{(0)}}$
A	co	15	0.25	−364	7.4	−2.6	0.35	−49
B	co	40	0.10	−188	2.1	11.8	5.60	−90
C	co	25	0.10	−90	13.9	−6.7	0.48	−6
D	co	10	0.05	−656	20.0	2.8	0.14	−33
E	post	25	0.10	80	−3.6	0.4	0.11	−22
F	post	15	0.07	−171	0.4	8.5	21.20	−428

the earthquake fault slip. The general features of the strain increment associated with the earthquake are tensile strain oriented normal to the Nankai trough with a magnitude of 5–20 ppm, with a smaller component of strain of about ±5 ppm oriented parallel to the trough. The principal strains derived from rectangular constant slip dislocation surfaces should reasonably approximate the true strain field except at points very close to or very far from the fault. Because the coastal relevel lines lie no closer than 20 km from the fault plane, we consider that fault end effects are negligible. We exclude strain changes farther than about one fault length from the main rupture, where our resolution becomes poor.

Thatcher and Rundle [1979] investigated the postseismic tide gage records and relevels to model the postseismic and interseismic processes between great earthquakes at the Nankai trough. They found that the immediate postseismic changes associated with the Nankaido earthquake can be adequately modeled by quasi-static or slow slip extending from the bottom of the seismic fault downdip for an additional 30 km within the lithosphere. The magnitude of the modeled postseismic slip comprises about 30–50% of the preceding coseismic slip. We use Thatcher and Rundle's model to calculate the horizontal strain field produced by the postseismic slip following the Nankaido earthquake. The salient features of the postseismic strain increment are compressive strain acting normal to the Nankai trough with a magnitude of 5–10 ppm and a small component of compressive or tensile strain aligned parallel to the trough. The fault parameters are listed in Table 1, and the model faults are shown in Figure 5.

We examined 4000 km of coseismic and postseismic resurveys [*Geographical Survey Institute of Japan*, 1954] within one fault length of the earthquake sources to identify regions of significant topographic relief. Because most of the survey routes are located along the coastline of Shikoku Island and the Kii Peninsula, only about 15%, or 650 km of the relevels, were performed over terrain that varied by more than 200 m. About 40% of these surveys show elevation dependent correlations of some kind; 30% display possible or ambiguous correlations, and 30% lack correlations in regions of topographic gradients. If topography does somehow localize deformation, this lack of ubiquity might be expected because the strain field is inhomogeneous, local topography is not always oriented favorably in the strain field, and mitigating factors such as three dimensionality may enter. The most striking correlations are shown in Figure 6, with the elevation change displayed above the topographic profile in each of the six cases, A–F. Also shown in Figure 6 are the calculated profiles of elevation change from *Ando* [1975] for the coseismic profiles and from *Thatcher and Rundle* [1979] for the postseismic changes. In each case shown, the elevation change profile departs from its

predicted or regional value at the topographic feature. The approximate value of $v^{(1)}/h$, or the ratio of peak-to-trough elevation change to the topographic height difference, accompanies the plots in Figure 6, and is listed in Table 2. Both $v^{(1)}$ and h are estimated departures from regional trends. The calculated principal strains at each of the five sites are shown in Figure 5.

We have attempted to assess the likelihood of significant measurement error in the Nankaido/Tonankai leveling data. Because the terrain in the area is quite steep (see Table 2), sight lengths were slope-limited and should have been nearly constant with time, minimizing refraction error [*Strange*, 1981; *Stein*, 1981]. Miscalibration of rods should be revealed by an exact bench mark-to-bench mark correlation of geodetic tilt and terrain slope, which is not observed at sites A, B, C, and D but is possible at E and F. Groundwater withdrawal can be ruled out because of subsidence that correlates with topographic highs rather than with basins.

Figure 7 shows the observed elevation change/topographic height $(v^{(1)}/h)$ values as a function of the predicted regional strain change $(e_{xx}^{(0)})$, the component of strain parallel to the level lines based on the calculated principal strains. The elastic model (equation (16)) predicts that these data should fall on a straight line through the origin, with a negative slope of order
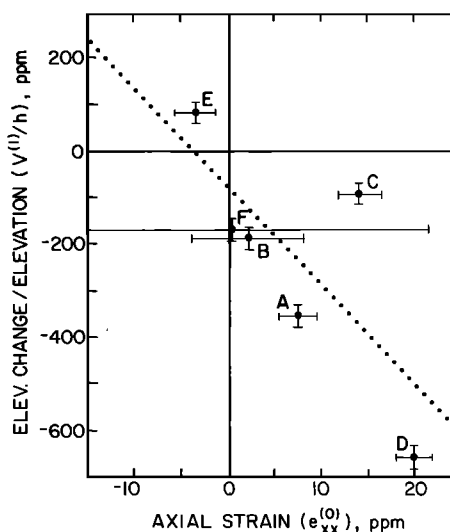

Fig. 7. Correlation $v^{(1)}/h$ versus modeled axial strain (equation (16)) for six localities in the Tonankai-Nankaido region. The dotted line indicates a linear regression. Local perturbation of vertical displacement $v^{(1)}$ and local relief h are estimated departures from regional trends. Error bars are based on $\sigma(v^{(1)}/h) = \pm 25$ ppm, σ (axial strain) $= (a^2 + b^2)^{1/2}$, where $a = 2$ ppm, $b =$ normal strain/axial strain.

unity. A linear regression of $v^{(1)}/h$ on $e_{xx}^{(0)}$ yields a slope -21, again showing that the observed tilt/slope correlation is at least an order of magnitude larger than that predicted by the elastic model.

Curiously, we note that the five localities that underwent extension all exhibit negative correlations, and the one (E) that underwent line-parallel compression does show a positive correlation. The data also show a discernible, although equivocal, trend toward larger $|v^{(1)}/h|$ with larger $|e_{xx}^{(0)}|$. Nonetheless, we must conclude that the elastic model does not account for a significant portion of the observed correlations.

Discussion and Conclusions

The widespread observation of correlations of level changes with topography suggests the need to assess the effect of an irregular free boundary on surface deformation. A simple elastic model based on the assumption of small slopes shows that topography indeed localizes both vertical displacements and horizontal strains. In particular, the model shows that topography will undergo local elevation-dependent uplift when subjected to far-field compression and, similarly, will experience elevation-dependent downdrop in extension.

Although this phenomenology is reminiscent of field observations, the predicted effects are very small. The localization of elastic deformation results in a ratio of perturbation displacement to elevation of the order of the regional strain. Thus we conclude that this mechanism can not contribute significantly to observed tilt/slope correlations in aseismic areas, which are often found to be as large as 10^{-4}. An example from southern California, where there are both leveling and nearby strain data available, confirms this discrepancy. For the much larger strains associated with the great Tonankai and Nankaido earthquakes, we still find elevation change to elevation ratios that are at least an order of magnitude larger than those predicted by the elastic model.

It is, nonetheless, intriguing to note that for the cases we examined where there exist leveling data in regions of topographic relief and directly measured or modeled strain data, all exhibit positive correlations in compression (one in California, one in Japan) or negative correlations in extension (one in California, five in Japan). This result may well be fortuitous given the paucity of available data, but we record it as a possible stimulus to further investigation. We note that additional correlations between elevation, gravity, and dilatation changes have been reported by *Jachens et al.* [1983].

The predicted topographic perturbation of surface strain (equation (15)), like the displacement, is also very small. However, it may in favorable circumstances be discernible with current distance and strain measuring technology. Recent results with a two-color geodimeter [e.g., *Langbein et al.*, 1982] indicate measurements precise to one part in 10^7. Equation (15) predicts a strain perturbation of the order of the characteristic slope times the regional strain. Topography with H/L of 10^{-1}, subjected to a regional strain of 10^{-6}, then, would give rise to a local perturbation strain of the order of 10^{-7}, which is at the limit of detection by the two-color geodimeter. Thus, in an area of steep relief that undergoes a relatively large far-field strain, the correlation given by (15) may be measurable in a bench mark-to-bench mark survey of horizontal strains. We are aware of no such detailed field studies but suggest that a monitoring program of this type may provide valuable insight into crustal deformation. The Sacks-Evertson borehole strainmeter has recorded earthquake strain

increments of 10^{-8}, and tidal strains smaller than 10^{-11} have been observed [*Sacks et al.*, 1981]. Placement of the strainmeters in regions of topographic gradients may substantially modify signal amplitudes. Equation (15) provides a first-order correction for this effect. It is interesting to note that while leveling and strain data are often regarded as independent and distinct, local topographic perturbations of both are directly linked.

References

Ando, M., Source mechanisms and tectonic significance of historical quakes along the Nankai trough, Japan, *Tectonophysics, 27,* 119–140, 1975.

Brown, L. D., and J. E. Oliver, Vertical crustal movements from leveling data and their relation to geologic structure in the eastern United States, *Rev. Geophys. Space Phys., 14,* 13–35, 1976.

Castle, R. O., J. D. Church, and M. R. Elliot, Aseismic uplift in southern California, *Science, 192,* 251–254, 1976.

Citron, G. P., and L. D. Brown, Recent vertical crustal movements from precise leveling surveys in the Blue Ridge and Piedmont provinces, North Carolina and Georgia, *Tectonophysics, 52,* 223–238, 1979.

Fitch, T. J., Plate convergence, transcurrent faults, and internal deformation adjacent to southeast Asia and the western Pacific, *J. Geophys. Res., 77,* 4432–4460, 1972.

Fitch, T. J., and C. H. Scholz, Mechanism of underthrusting in southwest Japan: A model of convergent plate interactions, *J. Geophys. Res., 76,* 7260–7292, 1971.

Geographical Survey Institute of Japan, Resurvey of the southwestern part of Japan after the great Nankaido earthquake of 1946, *J. Geogr. Surv. Inst. Jpn., 4,* 1–69, 1954.

Jachens, R. C., W. Thatcher, C. W. Roberts, and R. S. Stein, Correlation of changes in gravity, elevation and strain in southern California, *Science, 219,* 1215–1217, 1983.

Jackson, D. D., W. B. Lee, and C. Liu, Aseismic uplift in southern California: An alternative interpretation, *Science, 210,* 534–536, 1980.

Kanamori, H., Tectonic implications of the 1944 Tonankai and the 1946 Nankaido earthquakes, *Phys. Earth Planet. Inter., 5,* 129–139, 1972.

Kanamori, H., The energy release in great earthquakes, *J. Geophys. Res., 82,* 2981–2987, 1977.

Karcz, I., and U. Kafri, Geodetic evidence of possible recent crustal movements in the Negev, southern Israel, *J. Geophys. Res., 76,* 8056–8065, 1971.

Langbein, J. O., M. F. Linker, A. McGarr, and L. E. Slater, Observations of strain accumulation across the San Andreas fault near Palmdale, California, with a two-color geodimeter, *Science, 218,* 1217–1219, 1982.

Mark, R. K., J. C. Tinsley III, E. B. Newman, T. D. Gilmore and R. O. Castle, An assessment of the accuracy of the geodetic measurements that led to the recognition of the southern California uplift, *J. Geophys. Res., 86,* 2783–2808, 1981.

McKenzie, D. P., and R. L. Parker, The north Pacific: An example of tectonics on a sphere, *Nature, 216,* 1276–1280, 1967.

McTigue, D. F., and C. C. Mei, Gravity-induced stresses near topography of small slope, *J. Geophys. Res., 86,* 9268–9278, 1981.

Minster, J. B., and T. H. Jordan, Present-day plate motions, *J. Geophys. Res., 83,* 5331–5354, 1978.

Prescott, W. H., and J. C. Savage, Strain accumulation on the San Andreas fault near Palmdale, California, *J. Geophys. Res., 81,* 4901–4908, 1976.

Reilinger, R., Elevation changes near the San Gabriel fault, southern California, *Geophys. Res. Lett., 7,* 1017–1019, 1980.

Rundle, J. B., and M. McNutt, The Palmdale bulge: Is it or isn't it, *Eos Trans. AGU, 62,* 97–98, 1981.

Sacks, I. S., A. T. Linde, J. A. Snoke, and S. Suyehiro, A slow earthquake sequence followng the Izu-Ishima earthquake of 1978, in

Earthquake Prediction, An International Review, Maurice Ewing Ser., vol. 4, edited by D. W. Simpson and P. G. Richards, pp. 617–628, AGU, Washington, D. C., 1981.

Savage, J. C., W. H. Prescott, M. Lisowski, and N. E. King, Strain on the San Andreas fault near Palmdale, California: Rapid aseismic change, *Science, 211*, 56–58, 1981.

Sneddon, I. N., *Fourier Transforms*, McGraw-Hill, New York, 1951.

Stein, R. S., Discrimination of tectonic displacement from slope-dependent errors in geodetic leveling from southern California, 1953–1979, in *Earthquake Prediction, An International Review, Maurice Ewing Ser.*, vol. 4, edited by D. W. Simpson and P. G. Richards, pp. 441–456, AGU, Washington, D. C., 1981.

Strange, W. E., The impact of refraction correction on leveling inter-pretations in southern California, *J. Geophys. Res., 86*, 2809–2824, 1981.

Thatcher, W., and J. B. Rundle, A model for the earthquake cycle in underthrust zones, *J. Geophys. Res., 84*, 5540–5556, 1979.

D. F. McTigue, Fluid Mechanics and Heat Transfer Division I, Sandia National Laboratories, Albuquerque, NM 87185.

R. S. Stein, U. S. Geological Survey, 345 Middlefield Road, Menlo Park, CA 94025.